A Novel Dominant Mutation in *SAG*, the Arrestin-1 Gene, Is a Common Cause of Retinitis Pigmentosa in Hispanic Families in the Southwestern United States

Lori S. Sullivan,[1] Sara J. Bowne,[1] Daniel C. Koboldt,[2] Elizabeth L. Cadena,[1] John R. Heckenlively,[3] Kari E. Branham,[3] Dianna H. Wheaton,[4] Kaylie D. Jones,[4] Richard S. Ruiz,[5] Mark E. Pennesi,[6] Paul Yang,[6] David Davis-Boozer,[6] Hope Northrup,[7] Vsevold V. Gurevich,[8] Rui Chen,[9] Mingchu Xu,[9] Yumei Li,[9] David G. Birch,[4] and Stephen P. Daiger[1,5]

[1]Human Genetics Center, School of Public Health, The University of Texas Health Science Center, Houston, Texas, United States
[2]Nationwide Children's Hospital, Columbus, Ohio, United States
[3]Kellogg Eye Center, University of Michigan, Ann Arbor, Michigan, United States
[4]Retina Foundation of the Southwest, Dallas, Texas, United States
[5]Ruiz Department of Ophthalmology and Visual Science, McGovern Medical School, The University of Texas Health Science Center, Houston, Texas, United States
[6]Casey Eye Institute, Oregon Health and Science University, Portland, Oregon, United States
[7]Department of Pediatrics, McGovern Medical School, The University of Texas Health Science Center, Houston, Texas, United States
[8]Vanderbilt University, Nashville, Tennessee, United States
[9]Department of Molecular and Human Genetics, Baylor College of Medicine, Houston, Texas, United States

Correspondence: Stephen P. Daiger, Human Genetics Center, School of Public Health, P.O. Box 20186, Houston, TX 77225, USA; stephen.p.daiger@uth.tmc.edu.

LSS and SJB contributed equally to the work presented here and should therefore be regarded as equivalent authors.

Submitted: December 20, 2016
Accepted: April 23, 2017

Citation: Sullivan LS, Bowne SJ, Koboldt DC, et al. A novel dominant mutation in *SAG*, the arrestin-1 gene, is a common cause of retinitis pigmentosa in Hispanic families in the southwestern United States. *Invest Ophthalmol Vis Sci*. 2017;58:2774–2784. DOI:10.1167/iovs.16-21341

Purpose. To identify the causes of autosomal dominant retinitis pigmentosa (adRP) in a cohort of families without mutations in known adRP genes and consequently to characterize a novel dominant-acting missense mutation in *SAG*.

Methods. Patients underwent ophthalmologic testing and were screened for mutations using targeted-capture and whole-exome next-generation sequencing. Confirmation and additional screening were done by Sanger sequencing. Haplotypes segregating with the mutation were determined using short tandem repeat and single nucleotide variant polymorphisms. Genealogies were established by interviews of family members.

Results. Eight families in a cohort of 300 adRP families, and four additional families, were found to have a novel heterozygous mutation in the *SAG* gene, c.440G>T; p.Cys147Phe. Patients exhibited symptoms of retinitis pigmentosa and none showed symptoms characteristic of Oguchi disease. All families are of Hispanic descent and most were ascertained in Texas or California. A single haplotype including the *SAG* mutation was identified in all families. The mutation dramatically alters a conserved amino acid, is extremely rare in global databases, and was not found in 4000+ exomes from Hispanic controls. Molecular modeling based on the crystal structure of bovine arrestin-1 predicts protein misfolding/instability.

Conclusions. This is the first dominant-acting mutation identified in *SAG*, a founder mutation possibly originating in Mexico several centuries ago. The phenotype is clearly adRP and is distinct from the previously reported phenotypes of recessive null mutations, that is, Oguchi disease and recessive RP. The mutation accounts for 3% of the 300 families in the adRP Cohort and 36% of Hispanic families in this cohort.

Keywords: retinitis pigmentosa, dominant disease, SAG, Hispanic, arrestin-1

Retinitis pigmentosa (RP) is the most common form of inherited retinal disease (IRD) and has a prevalence of approximately 1 in 4000 worldwide.[1] It is characterized by night blindness and progressive loss of peripheral vision, often leading to complete blindness. The presence of pigmentary deposits, attenuated retinal vessels, and changes to the ERG are typical clinical findings.[2] RP is exceptionally heterogeneous, with more than 100 genetic causes already described (RetNet: https://sph.uth.edu/retnet/, in the public domain). Currently, mutations in 23 genes are known to cause dominant RP, 53 cause recessive RP, and 5 cause X-linked disease. At least 70 syndromic or systemic diseases include RP as a component. Variability in age of onset, secondary symptoms, rate of progression, and penetrance add to the complexity.

Our autosomal dominant RP (adRP) cohort, described previously,[3] currently consists of 300 well-characterized families with evidence of an autosomal dominant form of disease. Likely pathogenic mutations have been identified in 226 of these families (75%). Of the 300 families, 195 (65%) have dominant mutations in known adRP genes, 25 (8%) have X-linked mutations, 3 (1%) have multiple segregating muta-

tions, and 3 (1%) have dominant-acting mutations in genes previously associated with recessive diseases.

By a combination of exome sequencing and targeted-capture next-generation sequencing (NGS) of known IRD genes we identified a novel dominant-acting mutation in the *SAG* gene, a gene previously thought to cause only recessive disease.[4,5] This mutation (NM_000541.4:c.440G>T; NP_000532.2:p.Cys147-Phe) appears to descend from a common ancestor and accounts for 8 of the 74 families in the cohort in which mutations had not been identified previously.

Methods

Patient Ascertainment and Ophthalmologic Testing

This study adhered to the Declaration of Helsinki and was approved by the Committee for the Protection of Human Subjects at the University of Texas Health Science Center at Houston (UTHealth) as well as the institutional review board at each participating institution. Written informed consent was obtained from each participant before examination and genetic testing.

Patients in the adRP cohort have been ascertained over the past 25 years from collaborating clinicians at a variety of institutions. The subset of families described in this report was ascertained primarily at the Retina Foundation of the Southwest (Dallas, TX, USA); the Jules Stein Eye Institute, UCLA School of Medicine (Los Angeles, CA, USA); the Casey Eye Institute, Oregon Health and Science University, (Portland, OR, USA); and the Cizik Eye Clinic, UTHealth (Houston, TX, USA). Patients underwent detailed ophthalmologic examinations including best-corrected visual acuity, static visual fields (Humphrey), kinetic visual fields (Goldmann and Octopus), dark adaptometry, dark-adapted full-field ERGs, spectral-domain optical coherence tomography (SD-OCT), and fundus photography.[6]

Blood and/or saliva samples were collected from affected family members and additional relatives. Genomic DNA was extracted as previously described.[7,8]

Sanger Sequencing

Fluorescent di-deoxy Sanger sequencing was performed as previously described on a panel of adRP genes and exons containing mutation hotspots.[3,9–14] Additional Sanger sequencing was performed to confirm the results of NGS and to screen additional samples for the *SAG* mutation. Sanger sequencing was performed on a 3500xL DNA Sequencer (Applied Biosystems, Carlsbad, CA, USA).

Targeted-Capture Retinal Panels

Genomic DNA from each available family member was analyzed for the presence of mutations in retinal disease genes listed in RetNet (https://sph.uth.edu/retnet/, accessed June 1, 2016) using a targeted-capture NGS research protocol. Targeted capture was performed either in the Laboratory for Molecular Diagnosis of Inherited Eye Diseases, UTHealth, or at Baylor College of Medicine, as described previously[15] (Bowne SJ, et al. *IOVS* 2015;56:ARVO E-Abstract 1251).

Whole-Exome NGS Sequencing

Genomic DNA (1 μg) was used to make Illumina paired-end libraries according to the manufacturer's protocol (Illumina, Inc., San Diego, CA, USA), with modifications as described previously.[16,17] Exome capture was performed using a Nimblegen SeqCap EZ Human Exome Library v.2.0 (Roche, Madison, WI, USA) according to the manufacturers' protocols. Illumina paired-end sequencing (2 × 100 bp), alignment, and variant calling were performed as described previously.[18]

Bioinformatics

MendelScan[18] was used to rank single nucleotide variants (SNVs) and indels based on a combination of segregation, population frequency, retinal expression, and predicted functional impact. The Exome Aggregation Consortium (ExAC) data set (http://exac.broadinstitute.org/, in the public domain) and 1000 Genomes Database (http://www.1000genomes.org/, in the public domain) (both accessed December 12, 2016) were searched for the presence of the *SAG* p.Cys147Phe mutation. Variant Effect Predictor (http://www.ensembl.org/info/docs/tools/vep/index.html, in the public domain), which aggregates a number of different pathogenicity prediction algorithms including SIFT, PolyPhen-2, and Condel, predicted the pathogenicity of the *SAG* p.Cys147Phe mutation. Additional analyses using PROVEAN (http://provean.jcvi.org/, in the public domain) and MutationTaster (http://www.mutationtaster.org/, in the public domain) also were used. Multiple sequences were aligned using Clustal Omega (http://www.ebi.ac.uk/Tools/msa/clustalo/, in the public domain).

Haplotype Reconstruction

Haplotype analysis was done using short tandem repeat (STR) markers and SNVs identified as polymorphic from exome data and subsequent sequencing/typing in all samples. Specific markers included custom STRs and the following SNVs: rs80235307, rs7609436, rs2289475, rs4663420, rs4663420, rs181158151, rs745498, rs138961643, rs13018934, rs11563246, rs950834, rs4603827, and rs3731644. Genomic DNAs from all available family members were amplified, separated, and genotyped on a 3500xL DNA Sequencer (Applied Biosystems) as described previously.[16] STR alleles were determined using GeneMapper V3.7 (Applied Biosystems).

Molecular Modeling

The molecular effects of the mutation were predicted based on the 2.8-Å crystal structure of bovine arrestin-1.[19] Structures were obtained from the Research Collaboratory for Structural Bioinformatics Protein Data Bank (PDB: www.rcsb.org/pdb/, in the public domain). The structure (PDB ID: 1CF1) was visualized using ViewerPro 6.0 (Accelrys, San Diego, CA, USA). The effect of mutations on side chain clashes was determined using PyMOL software (available from pmol.org, distributed by Schrödinger, Cambridge, MA, USA).

Genealogy Inferences

Unstructured interviews with informative family members were conducted to determine the earliest known ancestors with vision problems consistent with RP, the general geographic locale of ancestral and living family members, and historical information on country or countries of origin. Pedigrees of contemporary family members and known ancestors were established in genetic counseling sessions (Fig. 1).

Results

Exclusion of Known Dominant Genes

Families in the adRP cohort in the Laboratory for Molecular Diagnosis of Inherited Eye Diseases, UTHealth, were ascer-

Investigative Ophthalmology & Visual Science

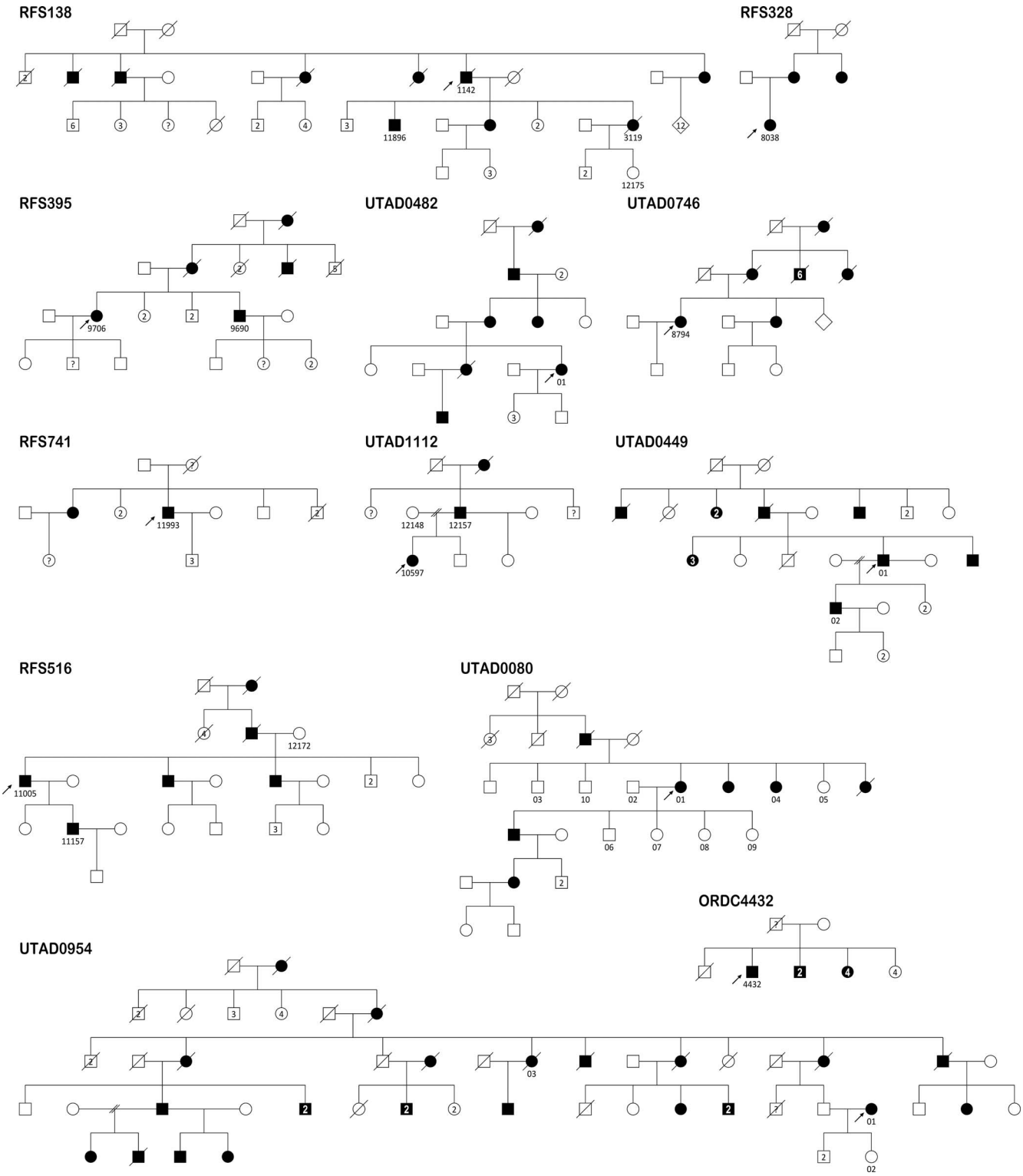

Figure 1. Pedigrees of families included in this study. Males are represented by *squares*, females by *circles*, multiple children of unknown sex by *diamonds*. Patients affected with RP are represented by *filled circles* or *squares*; numbered individuals were typed for the *SAG* mutation.

tained by clinical collaborators in several institutions. Families included in the cohort have a primary diagnosis of adRP by a knowledgeable retinal specialist and three or more disease generations or male-to-male transmission.[3] Earlier testing led to detection of the disease-causing gene in 75% of families, leaving 74 families without mutations in known genes.

Sanger sequencing of known dominant RP genes was negative in the remaining cohort families, including *RHO*, *PRPH2*, *PRPF31*, *RPGR*, *RP2*, and mutation hotspots in *HK1*, *IMPDH1*, *KLHL7*, *NR2E3*, *PRPF3*, *PRPF8*, *RP1*, *TOPORS*, and *SNRNP200*. Targeted-capture NGS using a large retinal disease gene panel confirmed these negative findings and extended

Investigative Ophthalmology & Visual Science

```
Human S-arrestin (SAG)      PTKLQESLLKKLGSNTYPFLLTFPDYLPCSVMLQPAPQDSGKSCGVDFEVKAFATD
Human β-arrestin 1 (ARRB1)  LTRLQERLIKKLGEHAYPFTFEIPPNLPCSVTLQPGPEDTGKACGVDYEVKAFCAE
Human β-arrestin 2 (ARRB2)  PTRLQDRLLRKLGQHAHPFFFTIPQNLPCSVTLQPGPEDTGKACGVDFEIRAFCAK
Human arrestin C (ARR3)     LTVLQERLLHKLGDNAYPFTLQMVTNLPCSVTLQPGPEDAGKPCGIDFEVKSFCAE
Mouse S-arrestin            LTQLQESLLKKLGDNTYPFLLTFPDYLPCSVMLQPAPQDVGKSCGVDFEVKAFASD
Cow S-arrestin              TTRLQESLIKKLGANTYPFLLTFPDYLPCSVMLQPAPQDVGKSCGVDFEIKAFATH
Frog S-arrestin             LTKVQERLMKKLGNNAFPFVLEFPDFLPCSVSLQPAPSDVGKACGVDFEIKAFSTN
Zebrafish S-arrestin        LTKVQEKLLRKLGDNAYPFFFEFPDNLPCSVGLQPAPKDVGKHCAVEFEVKAFCAE
Sea urchin β-arrestin       LTRLQERLIKKLGPNAYPFYFELPINSPSSVTLQPAPGDTGKPCGVDYELKTYVAE
Tunicate arrestin           KTRLQERLMKKLGEHSYPFFIDIPKDSPCSVTLQPAPGDTGKPCGVDYELKTYVWD
Roundworm β-arrestin        LSRLQERLKRKLGANAFPFWFEVAPKSASSVTLQPAPGDTGKPCGVDYELKTFVAV
```

Figure 2. Sequence alignment. Clustal alignment of arrestin sequences flanking *SAG* Cys147 from evolutionarily diverse members of the arrestin gene family. Conserved sequence of the structural 139-loop is shown in *green*, conservation of Cys147 in *yellow*. NP_000532.2:S-arrestin (*Homo sapiens*); NP_004032.2:beta-arrestin 1 isoform A (*H. sapiens*); NP_004304.1:beta-arrestin 2 isoform 1 (*H. sapiens*); NP_004303.2:arrestin-C (*H. sapiens*); NP_033144.1:S-arrestin (*Mus musculus*); NP_851343.1:S-arrestin (*Bos taurus*); NP_001081898.1:S-arrestin (*Xenopus laevis*); NP_956853.1:S-arrestin (*Danio rerio*); XP_011682264.1:beta-arrestin-1 isoform X1 (*Strongylocentrotus purpuratus*); NP_001041447:arrestin (*Ciona intestinalis*); NP_508183.1:probable beta-arrestin (*Caenorhabditis elegans*).

them to include all coding exons of *HK1*, *IMPDH1*, *KLHL7*, *NR2E3*, *PRPF3*, *PRPF8*, *RP1*, *TOPORS*, and *SNRNP200*.

No likely pathogenic variants were identified in the remaining 149 retinal disease–associated genes with the exception of a heterozygous p.Cys147Phe mutation in *SAG* (NM_000541.4:c.440G>T; NP_000532.2: p.Cys147Phe), which was originally classified as a variant of unknown significance. Exome testing in six cohort families also did not identify any likely pathogenic changes in known adRP genes nor in genes flanking the *SAG* mutation in chromosome band 2q37.1.

Identification of a Novel Dominant *SAG* Mutation

Exome sequencing of the unsolved cohort families provided an extensive list of potential disease-causing variants. Comparison across families identified a novel heterozygous variant in *SAG* that appeared in six independent families. Reexamination of previous gene-panel testing in families that had not undergone exome sequencing added an additional two cohort families with the identical *SAG* variant. The mutation had been disregarded earlier because of association of *SAG* with recessive disease. In all cases in which multiple affected family members were available, the mutation segregates with disease.

All eight families either self-identified as Hispanic or had common Hispanic surnames. We screened 52 additional Hispanic families from our noncohort collection for the presence of the *SAG* mutation and identified an additional three families. A fourth was found in a collaborator's collection, resulting in a total of 12 families. Across all 12 families, 20 affected individuals were tested and all were found to carry the mutation. No unaffected at-risk individuals were found with the mutation.

Pedigrees of representative families are shown in Figure 1.

Mutation Analysis

The *SAG* p.Cys147Phe mutation affects an amino acid that is conserved throughout the entire gene family of arrestins (Fig. 2). Alternative bioinformatic methods to predict protein impact yield nearly identical results: p.Cys147Phe is highly likely to be a deleterious mutation (Table 1). In databases of healthy control populations (e.g., ExAC, 1000Genomes), this variant appears once only, at a frequency of 1 per 120,594 alleles overall, and in 1 per 11,566 Hispanic alleles (ExAC database accessed December 14, 2016; http://exac.broadinstitute.org/). A collection of 4000+ genome sequences from Hispanic individuals in Texas was also queried and the variant was not found (Craig L. Hanis, PhD, School of Public Health, UTHealth, written personal communication, 2016).

Structural Analysis

The three-dimensional structure of mammalian arrestin-1 was solved at high resolution (PDB ID: 1CF1 for the basal conformation of the bovine protein[19] and 4ZWJ for the rhodopsin-bound mouse arrestin-1[20]). The cysteine at human position 147 (bovine position 143) is located in the center of the molecule, near the rhodopsin-binding finger loop and the 139-loop, a highly conserved feature[21] (Fig. 3). The small cysteine side chain faces inward and is in close contact with several neighboring hydrophobic residues (Fig. 3B). The replacement of this cysteine with the much bulkier phenylalanine is likely to affect protein folding: numerous side chain clashes (in particular with Leu132, Val247, Tyr255, and Ile323 in bovine arrestin-1, which correspond to Ile136, Val251, Tyr259, and Ile327, respectively, in the human protein) were detected by "mutating" this residue to Phe in PyMOL, regardless of the rotamer used.

Haplotype

Polymorphic SNVs and STRs were typed in all available individuals to identify the underlying haplotype on which the mutation likely arose. A region of 1.31 Mb, including the *SAG* mutation, is found in all affected individuals (Fig. 4). In several families, there is insufficient information to determine phase; however, all affected individuals have genotypes consistent with the inferred ancestral haplotype. No potential disease-causing mutations were detected in genes flanking SAG within the shared haplotype and no known genes causing retinal disease, other than *SAG*, are in this region. Thus, linkage disequilibrium with another potential disease-causing mutation is highly unlikely.

Table 1. Pathogenicity Prediction Results for *SAG* p.Cys147Phe Mutation

SIFT	PolyPhen	Grantham Distance	BLOSM62 Score	Condel Score	PROVEAN Score	Mutation Taster
0	1	205	−2	0.945	−10.92	Disease causing

Investigative Ophthalmology & Visual Science

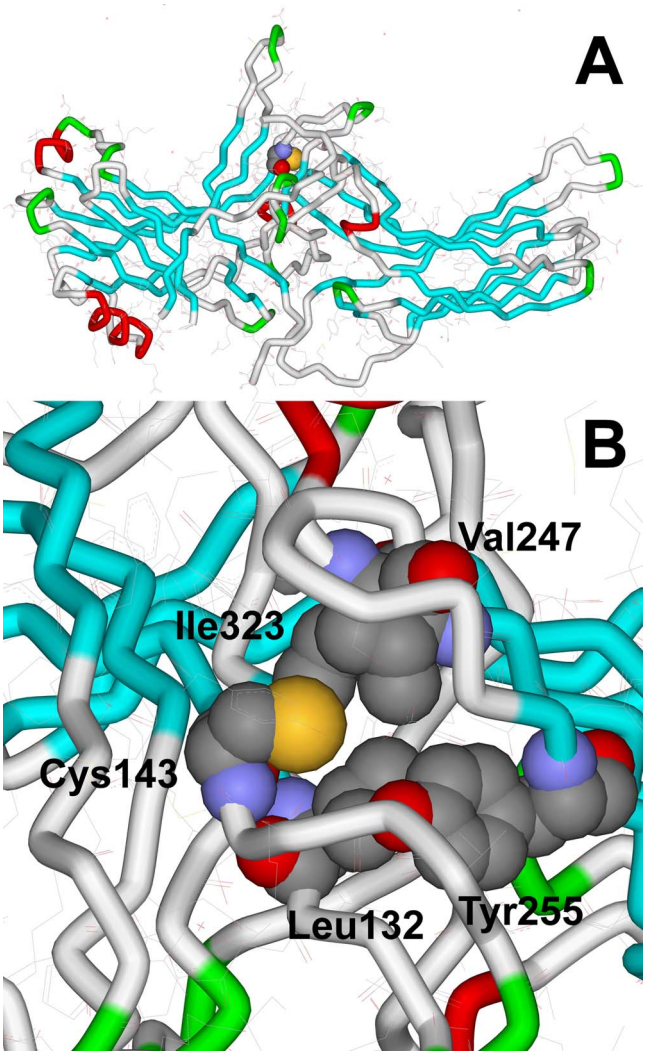

FIGURE 3. Cys147 in arrestin-1 structure. (**A**) Crystal structure of bovine arrestin-1 based on 1CF1.[44] The C-tail is not shown as it is not visible in any arrestin crystal structure. Molecule A is shown, with β-strands colored *light blue*, α-helices *red*, and β-turns, *green*. Cys143 (homologue of human Cys147) is shown as a Corey-Pauling-Koltun model. Here and in (**B**), carbon atoms are shown in *gray*, nitrogen in *blue*, oxygen in *red*, and sulfur in *yellow*. Note that the side chain is facing inward and Cys143 is localized near the rhodopsin-binding finger loop and the 139-loop (also known as the middle loop)[20] in the central crest of the molecule. (**B**) Intramolecular environment of Cys143 in bovine arrestin-1. Note tight packing around relatively small side chain of Cys143. Replacement of this cysteine with much bulkier phenylalanine creates clashes with indicated neighboring residues Leu132, Val247, Tyr255, and Ile323 (corresponding to residues Leu136, Val251, Tyr259, and Ile327 in highly homologous human arrestin-1).

Clinical Findings in Representative Patients and Families

Summary. Fourteen affected members of eight families underwent clinical examination (data summarized in Table 2). In the subset of families examined in Dallas, *SAG* mutations were found in 13 patients from seven families ranging in age from 26 to 67 (mean age = 48 years). Patients younger than 45 retained greater than 20/25 vision and, with one exception, retained at least 20/40 vision into their 60s. Rod ERGs were nondetectable in all but one patient tested at age 26, who retained a 4.0-μV response. Cone responses were reduced by 85% at age 45 and by 95% by age 60, consistent with the degree of field constriction. All patients showed elevations in final dark-adapted visual thresholds following 45 minutes of dark adaptation. Unlike in patients with Oguchi disease, extended (3 hours) dark adaptation did not lead to a further gain in sensitivity. None of the patients with *SAG* mutations showed the Mizuo-Nakamura phenomenon characteristic of Oguchi disease associated with recessive *SAG* mutations.[4] The fundus typically showed pigmentary changes characteristic of RP. In addition, several patients had multiple hyperreflective spots, which appeared on OCT to be distributed through all retinal layers (Fig. 5).

Family RFS138. A 51-year-old male presented with visual acuity loss to 20/200 OU. Rod ERGs were nondetectable and cone ERG responses were reduced greater than 95%. Visual fields measured 4 degrees in each eye. His final dark-adapted threshold with an 11-degree test centrally fixated was elevated by 3.3 log units. His daughter presented at age 28 years reporting peripheral vision loss and nyctalopia. Visual acuity was 20/15 OD and 20/50 OS. Her final dark-adapted threshold was elevated 0.9 log unit with an 11-degree test centrally fixated. Rod responses were minimally detectable and cone ERG responses were reduced by 90%. The proband's son was diagnosed with adRP at age 54 years with acuity reduced to 20/40 OU. Visual fields were constricted to 10 degrees. Rod ERG responses were nondetectable. Cone ERG responses were reduced by 85%. His final dark-adapted threshold was elevated by 3.4 log units with an 11-degree test centrally fixated. Bone-spicule pigment was present in the midperiphery and cystoid macular edema (CME) was evident on OCT.

Family RFS328. A 42-year-old female reported first noticing peripheral vision loss and night blindness at age 40 years. Visual acuity was decreased to 20/63 OD and 20/32 OS with nondetectable rod ERG responses and cone ERG responses reduced by 97%. Visual fields were constricted to 25 degrees' diameter and the final dark-adapted threshold was elevated 2.5 log units with an 11-degree, centrally fixated test. Severe bone-spicule pigment was present in the midperiphery with vessel attenuation and optic disc pallor.

Family RFS395. A 59-year-old male first reported noticing progressive peripheral vision loss, nyctalopia, and photophobia at age 53 years. Visual acuity was 20/40 OD and 20/25 OS with nondetectable rod ERG responses and cone responses reduced by 96%. Visual fields were constricted to less than 10 degrees and the final dark-adapted threshold was elevated by 0.8 log unit. The fundus showed peripheral pigmentation in all quadrants but minimal vessel attenuation. The patient's 45-year-old sister reported noticing symptoms only within the past year. Visual acuity was 20/32 OD and 20/32 OS. Rod ERGs were nondetectable and cone ERGs were reduced by 78%. Visual fields were constricted to 25 degrees. Her final dark-adapted threshold was elevated 0.6 log unit with an 11-degree test.

Family RFS516. A 48-year-old male first noticed field loss at age 24 and is aware of progressive field constriction. The patient retained 20/32 acuity in each eye with nondetectable rod ERGs and cone ERG amplitudes reduced by 98%. Visual fields were constricted to 15 degrees and the final dark-adapted threshold was elevated 1.0 log unit with an 11-degree test centrally fixated. Moderate bone-spicule pigment clumping was observed in the midperiphery along with arteriolar attenuation. The patient's 26-year-old son was also diagnosed with adRP and provided a DNA sample for analysis.

Family RFS741. A 59-year-old male first reported progressive peripheral vision loss beginning at age 51 years and severe night blindness since age 44 years. Acuity was reduced to 20/40 OU. Rod ERG responses were nondetectable with cone ERG responses reduced by 93%. Visual fields were constricted to 20 degrees with a temporal island in the periphery. The dark-

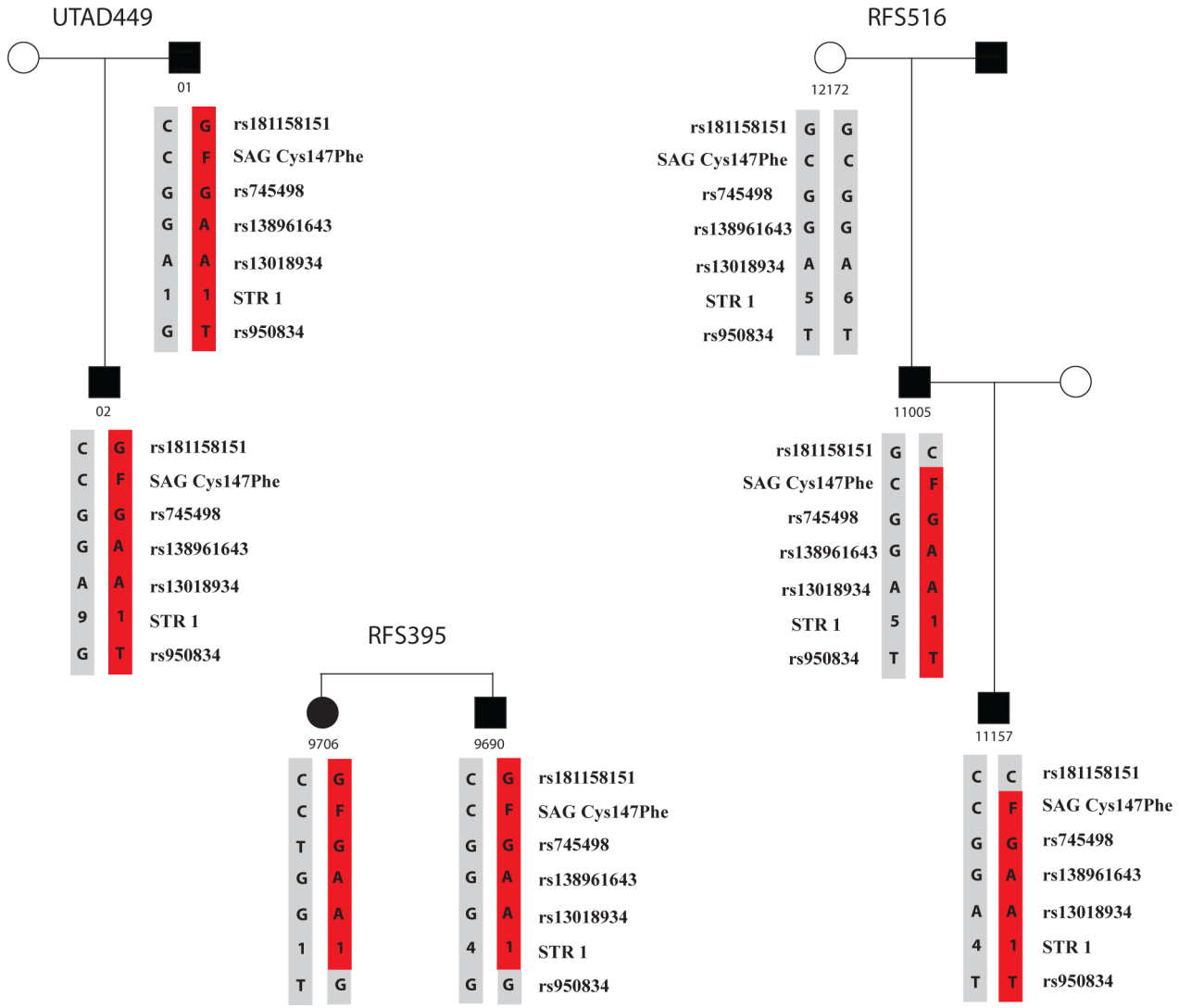

Figure 4. Haplotype surrounding the *SAG* Cys147Phe mutation. Seventeen single-nucleotide polymorphisms (SNPs) and four STRs were typed in all available members of the 12 families with the *SAG* Cys147Phe mutation. Genotypes were examined and the disease haplotype determined in as many families as possible. All individuals carried a haplotype or corresponding genotype consistent with a founder mutation occurring several generations ago. The minimal haplotype region was determined to be 1.31 Mb and located between SNPs rs181158151 and rs950834.

adapted threshold was elevated 3.6 log units. Moderate bone-spicule pigment was observed in the midperiphery along with atrophic areas in the mid-to-far periphery and optic disc pallor. Prominent CME was present OU in the macula.

Family UTAD0746. A 55-year-old female first noted decreasing night vision and restriction of peripheral vision at age 42 years. Visual acuity was 20/16 OD and 20/20 OS. Rod ERGs were nondetectable and cone ERGs were reduced by 62%. Visual fields were constricted to less than 20 degrees. The final dark-adapted threshold was borderline normal with an 11-degree test centrally fixated but elevated at least 2.0 log units elsewhere in the retina. The fundus showed moderate midperipheral bone spicules with pigmentary mottling in both eyes, but vessels showed minimal attenuation.

Family UTAD1112. A 41-year-old female first reported field loss at age 34 years and reported progressive peripheral vision restriction and nyctalopia. The patient retained 20/20 vision with nondetectable rod ERGs and cone ERG amplitude reduced by 96%. Visual fields were constricted to less than 20 degrees centrally, and the final dark-adapted threshold was elevated 0.5 log unit with an 11-degree test centrally fixated. Sparse bone-spicule pigment was observed in the midperiphery. The patient's 67-year-old father was also diagnosed with adRP, and retained 20/25 OD, 20/20 OS vision with non-detectable rod ERG responses. Cone ERGs to 30-Hz flicker were reduced in amplitude by 30% and significantly delayed in b-wave implicit time. Kinetic visual fields to spot size 3 were full, with a midperipheral scotoma in the superior field.

Family UTAD0080. A 45-year-old female with a family history consistent with dominant RP was first diagnosed at age 36. Visual acuity with correction was 20/40 OU with visual fields constricted to less than 10 degrees. On fundoscopy, scattered pigment clumps and a few bone spicules were seen throughout the retina. Some RPE atrophy in a lobule pattern was observed, especially in the temporal areas.

Family ORD4432. This 57-year-old male has a family history consistent with autosomal dominant inheritance. His visual acuity was 20/50 OD and 20/30 OS. Kinetic perimetry showed intact peripheral fields with midperipheral scotomas. Rod ERG responses were nondetectable. Cone responses showed moderate attenuation with delayed b-wave implicit times. His fundus showed moderate vessel attenuation,

Investigative Ophthalmology & Visual Science

Table 2. Clinical Description of Representative Patients

Patient ID	Diagnosis	Age at Examination	BCVA	VF	ffERG	DA Threshold Elevation, Log Units	Notes
RFS138-3119	adRP	28	20/15; 20/50	–	Rods reduced by 95%; cones reduced by 90% and delayed	1.0	
		31	20/30; 20/25	–	Rods reduced by 95%; cones reduced by 90% and delayed	0.6	
		40	20/25; 20/60	HVF 10°	Rods nondetectable; cones reduced by 98% and delayed	0.3	
RFS138-11896	adRP	54	20/40; 20/40	Kinetic 10°	Rods nondetectable; cones reduced by 85% and delayed	3.2	Diabetic
RFS138-1142	adRP	51	20/200; 20/200	Kinetic 4°	Rods reduced >95%; cones reduced by >99%	5.2	
RFS328-8038	Possible adRP	42	20/63; 20/32	HVF 25°	Rods nondetectable; cones reduced by 97% and delayed	2.5	
RFS395-9690	adRP	59	20/40; 20/25	HVF 10°	Rods nondetectable; cones reduced by 96% and delayed	0.6	
RFS395-9706	adRP	45	20/32; 20/32	HVF 25°	Rods nondetectable; cones reduced by 78% and delayed	0.4	
RFS516-11005	adRP	48	20/32; 20/32	HVF 15°	Rods nondetectable; cones reduced by 98% and delayed	1.1	Diabetic
		51	20/20; 20/25 (IOL at 49 y)	Kinetic 20° with peripheral islands		1.3	
RFS741-11993	Possible adRP	59	20/40; 20/40	Kinetic 20° with peripheral islands	Rods nondetectable; cones reduced by 93% and delayed	3.6	Foveal swelling OU
UTAD0746-8794	adRP	55	20/16; 20/20	HVF 20°	Rods nondetectable; cones reduced by 62% and delayed	0.0	
UTAD1112-10597	adRP	41	20/25; 20/25	HVF 20°	Rods nondetectable; cones reduced by 96% and delayed	0.5	Diabetic
UTAD1112-12157	adRP	67	20/25; 20/20	Full with midperipheral scotoma	Rods nondetectable; cones reduced by 30%	0.3	Diabetic
UTAD0080-01	adRP	42	Not done	HVF 12°	Nondetectable	1.4	
		45	20/40; 20/40	HVF 10°;	Nondetectable	2.0	
		63	20/200; 20/80	HVF <10°	–	–	
ORD 4432	adRP	57	20/50; 20/30	Full with midperipheral scotoma	Rods nondetectable; cones moderately reduced and delayed		

BCVA, best-corrected visual acuity; DA, dark-adapted; ffERG, full-field electroretinogram; VF, visual field; HVF, Humphrey visual field.

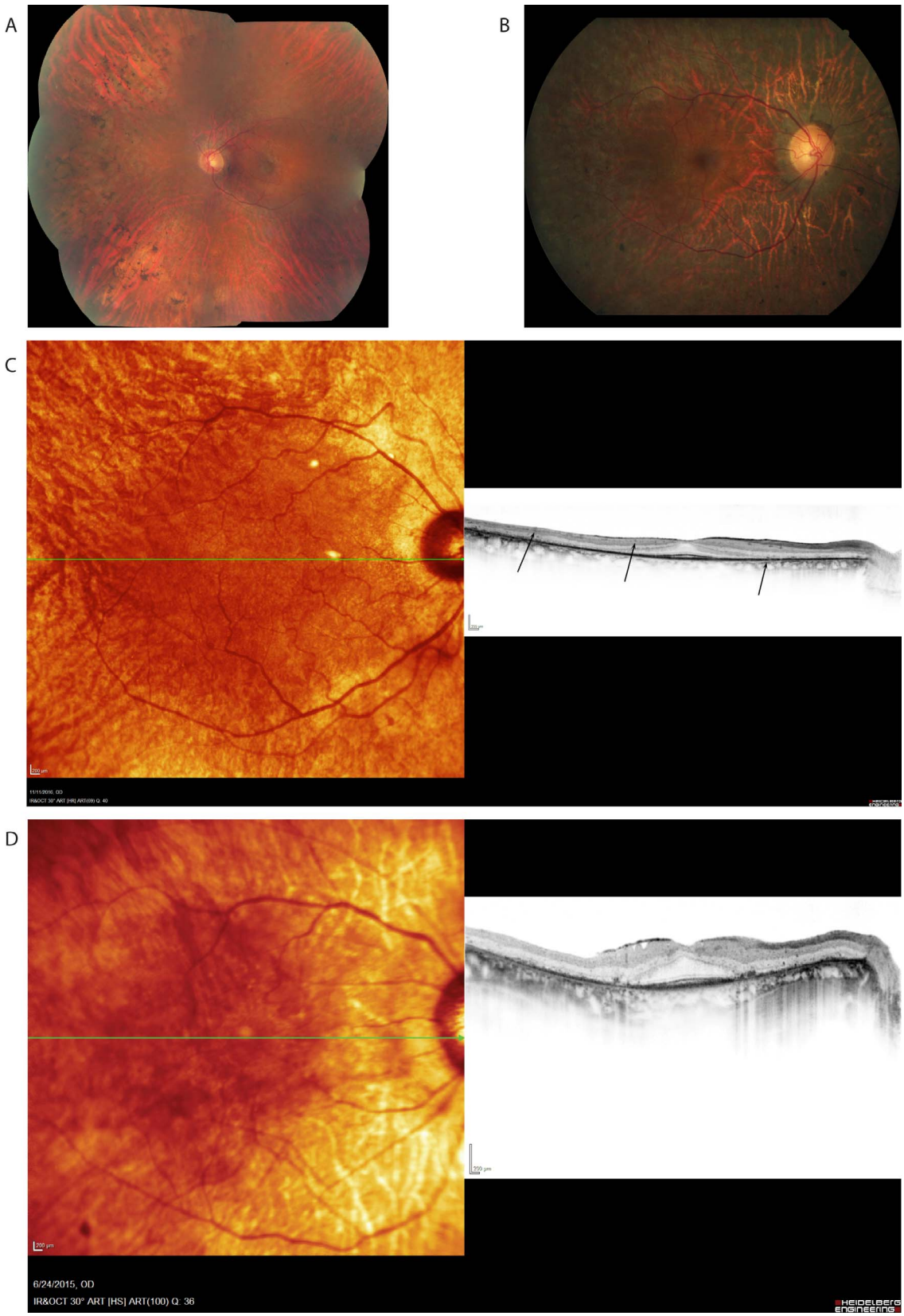

Figure 5. Fundus montages and OCTs of representative patients with the *SAG* Cys147Phe mutation. (**A**, **C**) Patient RFS516-11005, a 48-year-old male with adRP. Retinal thinning, bone-spicule pigmentation and patches of atrophy are present in a midperipheral ring. A horizontal midline OCT scan (**C**) shows an intact ellipsoid zone in the central macula but extensive degeneration outside the arcades. The *arrows* indicate hyperreflective spots, which are seen in all retinal layers. (**B**, **D**) Patient RFS 138-11896, a 54-year-old male with adRP. Extensive atrophy is present throughout the periphery. A horizontal midline OCT scan (**D**) shows an intact ellipsoid zone in the central macula. Immediately peripheral to the central macula there is loss of the photoreceptor layer, including the nuclear layer, and extensive disruption of the RPE.

Investigative Ophthalmology & Visual Science

pigment mottling in the macula, and a ring of depigmentation around the arcades.

Discussion

The p.Cys147Phe Mutation in *SAG* Is Common in Hispanic adRP Patients of Mexican Ancestry

The p.Cys147Phe mutation in *SAG* accounts for 36% of Hispanic families in our adRP cohort (8/22) and 3% of the overall total (8/300). Haplotype analysis is consistent with the hypothesis that the p.Cys147Phe mutation is the result of a founder mutation event and that all of the families are distantly related. Although families could not be linked by pedigree reconstruction, interviews of the oldest individuals indicated that many families had lived in what is now Texas for multiple generations, perhaps since the 1700s when the Spanish colonizers of Mexico established permanent settlements in the region via land grants.

In regions of the United States with large populations of Hispanic individuals of Mexican origin (e.g., Texas and California), it is likely to be a significant cause of disease, whereas in other parts of the country it may be less common among Hispanic individuals and rare otherwise. This is borne out by an earlier study of families with adRP from the Northeastern region of the United States,[22] where the Hispanic population is significantly smaller than in Texas or California and is also primarily of Caribbean and South American origin (U.S. Census Bureau Report C2010BR-04: http://www.census.gov/library/publications/2011/dec/c2010br-04.html). In that study, neither the p.Cys147Phe mutation nor any other pathogenic mutation in *SAG* was found. A recent study of 35 Hispanic RP probands, ascertained in Miami with origins primarily in Cuba, Colombia, and Puerto Rico, also did not report the *SAG* mutation.[23]

Dominant Mutations in a Recessive Gene

Before our finding, mutations in the *SAG* gene had been identified in only two human diseases: Oguchi disease,[4] a form of congenital stationary night blindness, and recessive RP.[5] Both diseases are recessive and all mutations are presumed to be functional nulls, resulting in absence of a functional protein. A single example of a patient with both an amino acid substitution and an exonic duplication has been reported, but without evidence of compound heterozygosity.[24] All previously reported pathogenic *SAG* alleles are nonsense or frameshift mutations, and heterozygous carriers are asymptomatic. Additionally, recessive canine retinal atrophy (PRA) in Basenji dogs has been attributed to a homozygous stop-loss mutation in *SAG*.[25]

Finding genes that harbor both dominant and recessive mutations is becoming more common. For IRDs, six genes have been identified (seven including *SAG*) with both dominant and recessive pathogenic mutations. *BEST1*,[26] *RHO*,[27] *RP1*,[28] and *RPE65*[16] cause both dominant and recessive RP; *IMPG1* mutations cause dominant and recessive macular degeneration,[29] and *GNAT1* can cause dominant or recessive congenital stationary night blindness (CSNB).[30]

Role of S-Antigen Visual Arrestin-1 in Phototransduction

S-antigen visual arrestin-1 is the second most abundant protein in rod photoreceptors, present at approximately 0.8:1 molar ratio to rhodopsin.[31,32] *SAG* is part of the highly conserved arrestin gene family and has homologues in species as evolutionarily distant as roundworms and tunicates[33] (Fig. 2). In humans (and all other mammals) the arrestin family is composed of four members: *SAG* (S-arrestin/S-antigen/arrestin-1), *ARR3* (cone arrestin/X arrestin), *ARRB1* (arrestin beta 1), and *ARRB2* (arrestin beta 2). *SAG* and *ARR3* are the visual arrestin genes and their expression is photoreceptor-specific,[34] whereas the two beta-arrestins are ubiquitously expressed.[33] Crystal structures for all four vertebrate subtypes are solved and they have a common two-domain structure with an extended carboxy-terminal tail[19,35–37] (Fig. 3). Extensive work has been done to map the functional properties of S-antigen visual arrestin-1 onto the three-dimensional structure and to delineate critical characteristics.

The primary function of S-antigen visual arrestin-1 in photoreceptors is well understood. Rods are sensitive to a single photon of light,[38] and it is crucial for the signaling cascade driven by rhodopsin, a G protein-coupled receptor, to be under tight control. After being activated by light, rhodopsin amplifies the signal by activating multiple transducin molecules, which in turn activate cyclic guanosine monophosphate (cGMP) phosphodiesterase. As the concentration of cGMP decreases in the rod outer segment, cGMP-gated cation channels close. To be ready for the next incoming photon, the rod cell must reset, and this occurs with a series of inactivation steps. The role of arrestin-1 is to bind to rhodopsin that has both been activated by light and also phosphorylated at specific serine and threonine residues in its C-terminus by rhodopsin kinase (systematic name GRK1). The binding of arrestin-1 to phosphorylated rhodopsin physically blocks transducin molecules from binding[39,40] and prevents subsequent steps in phototransduction from taking place, resulting in the timely return of the cell to its photosensitive state.

Analysis of the protein structure supports both pathogenicity and a likely mechanism of disease caused by the *SAG* Cys147Phe mutation. Replacement of the cysteine with the much larger phenylalanine is likely to perturb the tertiary structure to the point in which misfolding occurs, leading to protein aggregation and the unfolded protein response (UPR). This is analogous to the many dominant rhodopsin mutations that cause RP via protein misfolding.[41,42] Recessive mutations in *SAG* also may elicit the UPR by constitutive rhodopsin signaling[43] but perhaps at a slower rate, usually resulting in CSNB but sometimes causing progressive degeneration.[5,43] The presence of arrestin-1 in cones, as well as rods,[44] is likely to explain how cone function is also affected by this mutation.

Conclusions

The history of the *SAG* p.Cys147Phe mutation is intriguing, and its prevalence in American Hispanic individuals with adRP may be analogous to that of the rhodopsin p.Pro23His mutation in American non-Hispanic individuals.[45] If the mutation occurred in Spain, before the Spanish colonization of what is now Mexico and Texas, it may be prevalent in other parts of the world as well. Until now, the p.Cys147Phe mutation in the *SAG* gene has been consistently overlooked because it does not conform to our expectations: monoallelic variants found in the "canonical recessive genes" are routinely classified as variants of unknown significance, if they are annotated at all. Reanalysis of NGS data with fewer preconceived ideas of genotype/phenotype relationships may help in finding additional pathogenic genes and mutations for IRDs.

Acknowledgments

The authors thank Cheryl E. Avery for her highly skilled technical assistance and dedication to the project.

Investigative Ophthalmology & Visual Science

Supported by National Institutes of Health Grants EY007142 (SPD), EY009076 (DGB), EY011500 (VVG), EY010572 (MEP), and K08-EY026650 (PY); a Wynn-Gund TRAP Award (SPD); and grants from Foundation Fighting Blindness (SPD, DGB, MEP, PY), the William Stamps Farish Fund (SPD), the Hermann Eye Fund (SPD), the Max and Minnie Voelker Foundation (DGB), and an unrestricted grant to the Casey Eye Institute from Research to Prevent Blindness.

Disclosure: **L.S. Sullivan**, None; **S.J. Bowne**, None; **D.C. Koboldt**, None; **E.L. Cadena**, None; **J.R. Heckenlively**, None; **K.E. Branham**, None; **D.H. Wheaton**, None; **K.D. Jones**, None; **R.S. Ruiz**, None; **M.E. Pennesi**, None; **P. Yang**, None; **D. Davis-Boozer**, None; **H. Northrup**, None; **V.V. Gurevich**, None; **R. Chen**, None; **M. Xu**, None; **Y. Li**, None; **D.G. Birch**, None; **S.P. Daiger**, None

References

1. Daiger SP, Bowne SJ, Sullivan LS. Perspective on genes and mutations causing retinitis pigmentosa. *Arch Ophthalmol*. 2007;125:151–158.
2. Heckenlively JR. *Retinitis Pigmentosa*. Philadelphia, PA: J.B. Lippincott; 1988.
3. Sullivan LS, Bowne SJ, Birch DG, et al. Prevalence of disease-causing mutations in families with autosomal dominant retinitis pigmentosa: a screen of known genes in 200 families. *Invest Ophthalmol Vis Sci*. 2006;47:3052–3064.
4. Fuchs S, Nakazawa M, Maw M, Tamai M, Oguchi Y, Gal A. A homozygous 1-base pair deletion in the arrestin gene is a frequent cause of Oguchi disease in Japanese. *Nat Genet*. 1995;10:360–362.
5. Nakazawa M, Wada Y, Tamai M. Arrestin gene mutations in autosomal recessive retinitis pigmentosa. *Arch Ophthalmol*. 1998;116:498–501.
6. Bowne SJ, Sullivan LS, Wheaton DK, et al. North Carolina macular dystrophy (MCDR1) caused by a novel tandem duplication of the PRDM13 gene. *Mol Vis*. 2016;22:1239–1247.
7. Sohocki MM, Daiger SP, Bowne SJ, et al. Prevalence of mutations causing retinitis pigmentosa and other inherited retinopathies. *Hum Mutat*. 2001;17:42–51.
8. Bowne SJ, Sullivan LS, Koboldt DC, et al. Identification of disease-causing mutations in autosomal dominant retinitis pigmentosa (adRP) using next-generation DNA sequencing. *Invest Ophthalmol Vis Sci*. 2011;52:494–503.
9. Gire AI, Sullivan LS, Bowne SJ, et al. The Gly56Arg mutation in NR2E3 accounts for 1–2% of autosomal dominant retinitis pigmentosa. *Mol Vis*. 2007;13:1970–1975.
10. Bowne SJ, Sullivan LS, Gire AI, et al. Mutations in the TOPORS gene cause 1% of autosomal dominant retinitis pigmentosa. *Mol Vis*. 2008;14:922–927.
11. Friedman JS, Ray JW, Waseem N, et al. Mutations in a BTB-Kelch protein, KLHL7, cause autosomal-dominant retinitis pigmentosa. *Am J Hum Genet*. 2009;84:792–800.
12. Churchill JD, Bowne SJ, Sullivan LS, et al. Mutations in the X-linked retinitis pigmentosa genes RPGR and RP2 found in 8.5% of families with a provisional diagnosis of autosomal dominant retinitis pigmentosa. *Invest Ophthalmol Vis Sci*. 2013;54:1411–1416.
13. Bowne SJ, Sullivan LS, Avery CE, et al. Mutations in the small nuclear riboprotein 200 kDa gene (SNRNP200) cause 1.6% of autosomal dominant retinitis pigmentosa. *Mol Vis*. 2013;19:2407–2417.
14. Sullivan LS, Koboldt DC, Bowne SJ, et al. A dominant mutation in hexokinase 1 (HK1) causes retinitis pigmentosa. *Invest Ophthalmol Vis Sci*. 2014;55:7147–7158.
15. Wang F, Wang H, Tuan HF, et al. Next generation sequencing-based molecular diagnosis of retinitis pigmentosa: identification of a novel genotype-phenotype correlation and clinical refinements. *Hum Genet*. 2014;133:331–345.
16. Bowne SJ, Humphries MM, Sullivan LS, et al. A dominant mutation in RPE65 identified by whole-exome sequencing causes retinitis pigmentosa with choroidal involvement. *Eur J Hum Genet*. 2011;19:1074–1081.
17. Wang X, Wang H, Sun V, et al. Comprehensive molecular diagnosis of 179 Leber congenital amaurosis and juvenile retinitis pigmentosa patients by targeted next generation sequencing. *J Med Genet*. 2013;50:674–688.
18. Koboldt DC, Larson DE, Sullivan LS, et al. Exome-based mapping and variant prioritization for inherited Mendelian disorders. *Am J Hum Genet*. 2014;94:373–384.
19. Hirsch JA, Schubert C, Gurevich VV, Sigler PB. The 2.8 A crystal structure of visual arrestin: a model for arrestin's regulation. *Cell*. 1999;97:257–269.
20. Kang Y, Zhou XE, Gao X, et al. Crystal structure of rhodopsin bound to arrestin by femtosecond X-ray laser. *Nature*. 2015;523:561–567.
21. Vishnivetskiy SA, Baameur F, Findley KR, Gurevich VV. Critical role of the central 139-loop in stability and binding selectivity of arrestin-1. *J Biol Chem*. 2013;288:11741–11750.
22. Sippel KC, DeStefano JD, Berson EL, Dryja TP. Evaluation of the human arrestin gene in patients with retinitis pigmentosa and stationary night blindness. *Invest Ophthalmol Vis Sci*. 1998;39:665–670.
23. Zhang Q, Xu M, Verriotto JD, et al. Next-generation sequencing-based molecular diagnosis of 35 Hispanic retinitis pigmentosa probands. *Sci Rep*. 2016;6:32792.
24. Glockle N, Kohl S, Mohr J, et al. Panel-based next generation sequencing as a reliable and efficient technique to detect mutations in unselected patients with retinal dystrophies. *Eur J Hum Genet*. 2014;22:99–104.
25. Goldstein O, Jordan JA, Aguirre GD, Acland GM. A non-stop S-antigen gene mutation is associated with late onset hereditary retinal degeneration in dogs. *Mol Vis*. 2013;19:1871–1884.
26. Davidson AE, Millar ID, Urquhart JE, et al. Missense mutations in a retinal pigment epithelium protein, bestrophin-1, cause retinitis pigmentosa. *Am J Hum Genet*. 2009;85:581–592.
27. Rosenfeld PJ, Cowley GS, McGee TL, Sandberg MA, Berson EL, Dryja TP. A null mutation in the rhodopsin gene causes rod photoreceptor dysfunction and autosomal recessive retinitis pigmentosa. *Nat Genet*. 1992;1:209–213.
28. Khaliq S, Abid A, Ismail M, et al. Novel association of RP1 gene mutations with autosomal recessive retinitis pigmentosa. *J Med Genet*. 2005;42:436–438.
29. Manes G, Meunier I, Avila-Fernandez A, et al. Mutations in IMPG1 cause vitelliform macular dystrophies. *Am J Hum Genet*. 2013;93:571–578.
30. Naeem MA, Chavali VR, Ali S, et al. GNAT1 associated with autosomal recessive congenital stationary night blindness. *Invest Ophthalmol Vis Sci*. 2012;53:1353–1361.
31. Strissel KJ, Sokolov M, Trieu LH, Arshavsky VY. Arrestin translocation is induced at a critical threshold of visual signaling and is superstoichiometric to bleached rhodopsin. *J Neurosci*. 2006;26:1146–1153.
32. Hanson SM, Gurevich EV, Vishnivetskiy SA, Ahmed MR, Song X, Gurevich VV. Each rhodopsin molecule binds its own arrestin. *Proc Natl Acad Sci U S A*. 2007;104:3125–3128.
33. Gurevich EV, Gurevich VV. Arrestins: ubiquitous regulators of cellular signaling pathways. *Genome Biol*. 2006;7:236.
34. Nikonov SS, Brown BM, Davis JA, et al. Mouse cones require an arrestin for normal inactivation of phototransduction. *Neuron*. 2008;59:462–474.
35. Han M, Gurevich VV, Vishnivetskiy SA, Sigler PB, Schubert C. Crystal structure of beta-arrestin at 1.9 A: possible mechanism

Investigative Ophthalmology & Visual Science

of receptor binding and membrane Translocation. *Structure*. 2001;9:869–880.

36. Sutton RB, Vishnivetskiy SA, Robert J, et al. Crystal structure of cone arrestin at 2.3A: evolution of receptor specificity. *J Mol Biol*. 2005;354:1069–1080.
37. Zhan X, Gimenez LE, Gurevich VV, Spiller BW. Crystal structure of arrestin-3 reveals the basis of the difference in receptor binding between two non-visual subtypes. *J Mol Biol*. 2011;406:467–478.
38. Baylor DA, Lamb TD, Yau KW. Responses of retinal rods to single photons. *J Physiol*. 1979;288:613–634.
39. Wilden U. Duration and amplitude of the light-induced cGMP hydrolysis in vertebrate photoreceptors are regulated by multiple phosphorylation of rhodopsin and by arrestin binding. *Biochemistry*. 1995;34:1446–1454.
40. Krupnick JG, Gurevich VV, Benovic JL. Mechanism of quenching of phototransduction. Binding competition between arrestin and transducin for phosphorhodopsin. *J Biol Chem*. 1997;272:18125–18131.
41. Colley NJ, Cassill JA, Baker EK, Zuker CS. Defective intracellular transport is the molecular basis of rhodopsin-dependent dominant retinal degeneration. *Proc Natl Acad Sci U S A*. 1995;92:3070–3074.
42. Chapple JP, Grayson C, Hardcastle AJ, Saliba RS, van der Spuy J, Cheetham ME. Unfolding retinal dystrophies: a role for molecular chaperones? *Trends Mol Med*. 2001;7:414–421.
43. Wang T, Chen J. Induction of the unfolded protein response by constitutive G-protein signaling in rod photoreceptor cells. *J Biol Chem*. 2014;289:29310–29321.
44. Nikonov SS, Brown BM, Davis JA, et al. Mouse cones require an arrestin for normal inactivation of phototransduction. *Neuron*. 2008;59:462–474.
45. Dryja T, McGee TL, Hahn LB, et al. Mutations within the rhodopsin gene in patients with autosomal dominant retinitis pigmentosa. *N Engl J Med*. 1990;323:1302–1307.

Investigative Ophthalmology & Visual Science